Outflows from Massive YSOs as Seen by the Infrared Array Camera

Howard A. Smith, J. L. Hora, M. Marengo
Harvard-Smithsonian Center for Astrophysics, 60 Garden Street, Cambridge, MA 02138
hsmith@cfa.harvard.edu
and
Judith L. Pipher
Department of Physics and Astronomy, University of Rochester, Rochester, NY 14627

ABSTRACT

The bipolar outflow from the massive star forming cluster in DR21 is one of the most powerful known. Its extensive western lobe is particularly straightforward to study because it is has broken out of its massive natal molecular cloud and is conveniently oriented nearly normal to our line-of-sight. In *Spitzer* IRAC images of the DR21 region, the outflow stands out by virtue of its brightness at 4.5 :m (Band 2). Indeed, IRAC images of many galactic and extragalactic star formation regions feature prominent Band 2 morphologies. We have analyzed archival ISO SWS spectra of the DR21 outflow, including previously unpublished spectra, and compare the results with new H_2 shocked and UV-excitation models. H_2 line emission - not emission from dust, atoms, or PAH features - dominates the flux in IRAC at 4.5 :m , 5.8 :m and 8.0 :m, and is a significant contributor to the 3.6 :m (Band 1) flux as well. The new models and the measured IRAC fluxes across the outflow confirm that the DR21 outflow contains multiple shock excitation conditions. The results imply that IRAC images can be a powerful detector of, and diagnostic for, outflows caused by massive star formation activity in our galaxy, and in other galaxies as well. The results suggest that IRAC color-color diagnostic diagrams for star formation regions may need to take into account the possible influence of these strong emission lines. IRAC images of the general ISM in the region, away from the outflow, are in approximate but not precise agreement with theoretical models.

Subject headings: ISM: individual (DR21) – ISM: jets and outflows – ISM: molecules – infrared: ISM – stars: formation

Online material: color figures

1. INTRODUCTION

DR21 contains one of the most massive star formation regions and molecular outflows in our galaxy. It is an excellent test bed for studying the conditions of massive star formation, and for comparing competing ideas about the formation and subsequent evolution of massive new stars and their environments, for example, the relative roles of cloud collisions and fragmentation in these processes. The extended DR21 nebula consists of a filamentary ridge of massive star-forming clusters that stretch from DR21(main) northward to W75N, and includes clusters around the bright maser source DR21(OH). Along with the rest of the Cyg X complex in which it is embedded, DR21 appears as part of a shell-like structure around the super-massive Cyg OB2 association. This association lies in the direction of a tangent to the Orion arm of the Galaxy, and as a result its distance is relatively difficult to estimate. Dame, using CO and HI maps of the galaxy, estimates the distance to Cyg OB2 as 1.7kpc (private communication; Butt et al. 2003). We adopt this value for DR21 even though the most commonly used distance in the past literature has been 3 kpc. We thus revise downward a number of earlier estimates of luminosity, etc, so as to scale accurately to this closer distance.

The giant molecular outflow in DR21 is one of the most powerful outflows in our galaxy. An estimated driving force (estimated from the H_2 lines) of ~5.5 10^{30} dynes (Garden et al. 1986) exceeds the driving force of the Orion-Irc2 outflow by almost a factor of 6 (Cabrit & Bertout 1992). The outflow velocity of about 60 kms^{-1} or more drives a mass estimated at >3000M_O. The energy of the flow is in excess of $2x10^{48}$ ergs; the luminosity of the two-micron H_2 flow alone has been calculated to be 1800 L_O, and, as we show below, the 2 :m lines are not even the brightest ones. Cyganowski, *et al.* (2003) claim evidence for a second "highly collimated" flow perpendicular to the main one. In part because of the distance to DR21, and also because of the high extinctions there, our understanding of the complex has been somewhat limited. That DR21 has regions of very high extinction was shown by Chandler, Gear, and Chini (1993) and Chandler *et al.* (1993), who use the 1.3-mm dust and CS line observations, respectively, to conclude that clumps exist with column densities as high as $N(H+H_2)$~$3x10^{24}$ cm^{-2} ; $C^{18}O$ observations (Wilson and Mauersberger, 1990) had provided estimate that were also substantial but about ten times less. Adjusting to the closer distance of 1.7kpc and converting to visual extinctions give an estimate in places of Av~1000. *Spitzer* IRS data on the embedded young protostar finds a very deep CO_2 absorption also consistent with this estimate (Smith *et al.* 2006, in prep.). The IRAS satellite detected a very bright point source near the apparent source of the massive outflow, but identifying the actual source of the flow, a massive YSO, has proved elusive. Previous studies of the outflow region identified a source "IRS1" as the driver for the outflow, but IRAC images find no point source coincident with the IRAS location. Instead, we find one overwhelmingly strong 8.0 :m (Band 4) point source located about 10" from the position of the K-band star first dubbed "IRS1"(Davis and Smith 1996). This IRAC source was undetected at K; it is a young ~O7 star with L_{FIR} ~ 1.5 $x10^5$ Lo, apparently still accreting from its envelope; a full description of the source and its environment is in Smith *et al.* (*2006 op cit*). It is this source which is thought to power the immense bipolar outflow from the cloud.

The outflow has been imaged and studied in H_2 by numerous authors (e.g., Garden *et al.* 1986;

Garden *et al.* 1990; Davis & Smith 1996; and Fernandes *et al.* 1997). Fernandes *et al.* conclude that the 2:m line ratios are best fit by a PDR model with FUV field in the range of 2<g<3 and a preshock density of $n = 3x10^3\,cm^{-3}$. Smith *et al.* (1998) used the Infrared Space Observatory's Short Wavelength Spectrometer (ISOSWS) to analyze five lines between 4.9 :m and 17 :m in one bright section of the outflow. They conclude there are both J and C-type shocks at work in the region, and distinguish this gas from the uv-excited gas at 2 :m modeled by Fernandes, Brand, and Burton.

In this paper we present new IRAC images of the outflow region which dramatically reveal at 4.5:m the structures seen by the 2μm images at much higher spatial resolution. The original IRAC observations of this region (Marston *et al.* 2004) were partially saturated on the bright point sources, with some effect on the neighboring outflow region pixels; our new observations were taken in HDR mode. We also present and analyze archival ISOSWS spectra of the DR21 outflow, material not published in the original Smith, Eisloffel and Davis (1998) paper; we report the fluxes on an additional four H_2 lines as well as the on the atomic hydrogen Brα recombination line, and limits to other line fluxes and features falling in nearly all of the wavelength coverage of the IRAC instrument. The results show that the *Spitzer* IRAC instrument is a superb probe of shocked structures because of the strength of the H_2 lines and the IRAC bandpasses.

2. OBSERVATIONS AND ANALYSIS

2.1 *IRAC Observations of the Outflow*

The original DR21 IRAC observations were taken as an Early Release Observation (ERO) and published in Marston *et al.* (2004). We repeated those observations in HDR (and subarray) mode in regions around the bright point source and the outflow that had suffered from saturation effects. A full description of the point source and its nature will be presented elsewhere (Smith *et al.* 2006). The data analyzed here were processed in pipeline S11.0.2. Figure 1 shows the IRAC 3.6 :m / 4.5 :m /8.0 :m (Band 1,2,4) color composite of the western lobe of the outflow region. Superimposed on the image is the placement of the ISOSWS beam for the primary spectral observation, TDT 04402144 - it is this region of the shock which we analyze in detail below.

Davis and Smith (1996) obtained high resolution, high SNR images of the H_2 1-0 S(1) line emission from DR21. It was this same Davis and Smith paper which most convincingly identified a bright 2 :m star as the source of the outflow. As we show in more detail (Smith *op cit*) this is an erroneous identification, and the actual driving star is located about 15arsec away; it is not apparent in any K-band images, but dominates the entire region at 8 :m. Davis and Smith used a narrow-band ()8 = 0.02 :m) filter centered at 2.12 :m to obtain their H_2 image, and also a wide-band K filter, and subtracted the scaled K-band image from the narrow-band image to produce the line map. Their spatial resolution was 0.63 arcsec/pixel. In Figure 2 we superimpose the contours of their 1-0 S(1) image on our (lower resolution) IRAC 4.5 :m (Band 2) image. There is a nearly exact correspondence between the H_2 peaks and filaments and the 4.5 :m structures. This close correspondence across the ~1 parsec length of the flow suggests

that the conclusions we draw from an analysis of the smaller ISOSWS field can be safely generalized to the entire shocked outflow.

2.2 *Infrared Space Observatory's Short Wavelength Spectrometer Observations*

ISOSWS obtained four sets of observations of the DR21 "West Lobe" in addition to another nine observations centered elsewhere around in the outflow region. Wright, Zimmermann, and Drapatz (1997) published an initial SWS analysis of the outflows in a short abstract, and concluded a combination of multiple shock components and some uv excitation were probably at work. Smith, Eisloffel, and Davis (1998) analyzed and published the results from one of the outflow observations, TDT 34700904, in their meticulous analysis of the H_2 emission from DR21 West. That SWS observation, which was not a full wavelength scan but rather a set of individual line scans, covered and obtained data on five of the H_2 lines: the 0-0 S(1) at 17.03 :m, and four that fall in the IRAC coverage: the 0-0S(5) and 0-0S(7) lines, and the 1-1 S(7) and 1-1 S(9) lines. We reanalyzed that dataset, and are in agreement with all of their figures. Based on the observed line strengths, and combined with 2 :m observations of H_2, Smith, Eisloffel, and Davis concluded that the excitation in the DR21 outflow could not be produced by a simple C- or J-shock, and a range of shock strengths was needed. This conclusion was in contrast to the results of Fernandes, Brand, and Burton (1997), who relied on ground-based observations (only) to argue that the H_2 lines in the DR21 outflow were best fit by a PDR model with FUV field in the range of $2<g<3$ and pre-shocked density $n>3x10^3$ cm^{-3}. Smith and Rosen (2004) extended the Fernandes, Brand and Burton analysis to simulate the *expected* images from IRAC observations under a wide range of shocked conditions.

We examined all four sets of ISOSWS observations of the DR21 West lobe outflow in an effort to try to understand the IRAC images more precisely. None of the SWS scans provided full, contiguous coverage. TDT 04402042 emphasized wavelengths over 10 :m, TDT 04402144 (figure 3a shows this spectral scan in the 7 - 8.8 :m interval) was contiguous from about 6.5 to 9.5 :m, and TDT 19301741 consisted of a series of some twenty-one short line scans between 2.2 :m and 36 :m. All were taken at different epochs and included slightly different portions of the brightest part of the outflow, but all were centered roughly on the same part of the outflow, differing only by about 10"; the latter TDT also used a larger beamsize, 20"x33". None of these differences have any substantial effect on our rather general conclusions.

The new TDTs we analyze here provide high SNR fluxes on four *additional* H_2 lines in the IRAC wavelength coverage beyond the five analyzed in the Smith, Eisloffel, and Davis study: the 0-0 S(9) and 0-0 S(11) lines, the 1-1 S(5) line, and the 1-0 O(5) line. In addition, SWS detected the weak hydrogen recombination line Br" line at 4.052 :m. Table 1a lists all of the observed H_2 lines from all the ISOSWS observations, and the fluxes in the ISO beam. The IRAC instrumental response is described in the IRAC Data Handbook (Section 5.2). We converted each of the observed line strengths into a flux density in the appropriate IRAC band. We find that in the 4.5 :m, 5.8 :m, and 8.0 :m bands the observed line strengths are enough to account for most of the measured IRAC fluxes in the outflow region studied by SWS (as indicated on Figure 1). The slight discrepancies, are within the errors of the respective measurements, for example due to slight rotations in the SWS beam between lines, with some modest corrections for the cumulative contributions of some of the weaker and more model dependent H_2 lines. Our

conclusion is that the IRAC 4.5 :m, 5.8 :m, and 8.0 :m bands 4 fluxes are dominated by H_2 line emission.

2.3 *The Weak Continuum; Faint or Unseen Features, CO and Br* "

The ISOSWS spectral scan of the bright outflow in the 7 - 8.8 :m interval is presented in Figure 3a. The H_2 0-0 S(4) line clearly dominates this interval. Also worthy of notice is the extremely faint continuum on which the line sits, only about 0.93 ±0.06 Jy – for comparison, the flux density in the H_2 0-0 S(4) line itself, as seen with IRAC 8.0 :m, is 0.37Jy. The H_2 0-0 S(5) line at 6.907:m also falls in the 8.0 :m window, and contributes 0.76Jy, making a total line flux density of 1.13 ± 0.1 Jy; the observed 8.0 :m flux density is 1.08Jy. The complete absence of any sign of PAH emission in Figure 3a is striking. For comparison, Figure 3b shows the spectrum of the bright region in DR21 around the driving source about 40arsec away. Here the strong PAH features completely dominate the spectrum, and the H_2 0-0S(4) line, though present, is peripheral. Figure 3b also shows clearly the emission lines from [ArII] 6.985 :m, [ArIII] 8.991 :m , and the HeII 12-10 line at 7.46 :m, that are excited by the embedded O star (Smith *et al., op cit*). The results confirm that in the outflow region of DR21 the H_2 lines dominate the IRAC 4.5 :m, 5.8 :m, and 8.0 :m band fluxes. Figure 4 plots the measured 4-band IRAC flux densities summed over the region equivalent to the ISOSWS beam, and compares them to the contributions from the observed ISOSWS H_2 lines in those IRAC bands. The observed H_2 lines, to within the uncertainties, can account for close to100% of the observed IRAC 4.5 :m, 5.8 :m, and 8.0 :m band fluxes in the outflow. In the IRAC 3.6 :m band the observed H_2 lines provide only about 50% of the observed IRAC flux density, with the remainder coming presumable from the continuum features at 3.6 :m.

Geballe & Garden (1990) used UKIRT to obtain spectra of the Orion shocked outflow at 4.74:m, the wavelength of the CO 1-0 P(8) line. They find it has a strength about 1/10 of the strength of the H_2 0-0 S(9) line there, and conclude, in agreement with some earlier observers, that shocked CO is an important contributor to the emission in the Orion outflow. Van Dishoeck *et al.* (1998) publish an ISOSWS scan of the Orion IRc2 region, which includes the region studied by Geballe and Garden; they report "possibly" seeing CO emission in the 4.4 - 4.8 :m region. In the ISOSWS scans of the DR21 West outflow, however, no CO lines are detected to a limit of about 3×10^{-16} Watts/m^2 – less than about 16% of the nearby H_2 0-0 S(9) line.

IRAC images of star formation regions and other nebulosity-rich objects often reveal strong 4.5 :m band emission, which is easily spotted as bright green nebulosity in 3-color IRAC images in which the 4.5 :m band is coded (typically) as green. Churchwell *et al.* (2004), in their analysis of reflection nebula RCW 49, see just such bright 4.5 :m band emission. They conclude that the atomic hydrogen Br" line at 4.052 :m provides about 20% of the nonstellar flux in the 4.5 :m band , dominating the extended emission in that source. In the case of DR21, however, we measure the Br" line with SWS to be 1.6 ±0.4 $\times 10^{-16}$ Watts/m^2, making it among the weakest of the 4.5 :m band lines in the outflow, and 10 times weaker than the H_2 0-0 S(9) line. No other hydrogen recombination lines are seen in the SWS spectra of the outflow lobe. We conclude that "green nebulosity," insofar as it resembles shocked outflows like DR21, signifies the presence of H_2 , not Br".

3. SHOCK VS. PDR MODELS OF H_2 EMISSION

3.1 *Shock vs. PDR models of the Outflow*

There are about 140 emission lines of H_2 in the IRAC bands whose strengths, depending on the model details, are within 1% of the strength of the strongest line in each excitaion case. Michael Kaufman and Mark Wolfire have provided us with their as yet unpublished results of updated PDR and shock models (Kaufman *et al.* 2005; see also Kaufman & Neufeld, 1996, and Wolfire *et al.* 1990). Figure 5a plots the brightest H_2 lines in the IRAC bands for the case of a preshocked density of $1x10^4$ cm^{-3} moving with one of eight different velocities. As might be expected, the strongest velocities produce by far the strongest line emission. It is also notable that the strongest velocities have the *least* flux variation between IRAC bands, whereas the weaker velocities produce emission lines whose contributions between the IRAC bands vary more substantively. Figure 5b sums the transmission-weighted line contributions of the shocked H_2 lines to each of the four bands, and plots their cumulative values in terms of IRAC band flux densities. Three different preshock densities and four different velocities are considered. The results illustrate that, in the case of v=25 kms^{-1} shocks, the 3.6 :m band and 4.5 :m band are relatively weak, while for higher velocity shocks the flux densities in the 4.5 :m band, especially, is the strongest of the four bands. This increase in the relative importance of the 4.5 :m band (and the 3.6 :m band) flux occurs because these bands include a considerably larger number of weaker lines which are excited more effectively only at higher velocities.

Fernandes *et al.* (1997), in their earlier analyses of ground-based observations of the DR21 outflow, concluded that the DR21 H_2 line ratios were best fit by PDR models because of the strength of the lines originating from the upper state v=2, 3, and 4 levels; these are preferentially populated via non-thermal mechanisms. We have obtained new H_2 PDR calculations from Wolfire and Kaufman (private comm; see Kaufman *et al.*, and Lehman, 1999, for a description of their method). Figure 6a plots all of the bright H_2 lines predicted in the IRAC bands for five different cases of density n and ultraviolet flux g (where g is the log of the flux in units of the local interstellar FUV radiation, taken as $2x10^{11}$ photons/sec-m^2). Figure 6b, an analog to Figure 5b for shocks, plots the accumulated flux density as it would be seen by IRAC from all these lines, in each of these five situations. The strongest emission obviously comes from the most dense, highest uv regions, with the 8.0 :m band being the brightest and 3.6 :m band the faintest. It is noteworthy, however, that at lower, more common densities and uv fields the most flux emerges in IRAC 4.5 :m band, not the 8.0 :m band. Fernandes, Brand, and Burton conclude from their data that the most likely excitation in DR21 is from a FUV field with 2#g#3 and a preshock density of n$3x10^3$ cm^{-3}.

The four new H_2 lines in DR21 we present here, the 0-0 S(9), 0-0 S(11), 1-1 S(5), and 1-0 O(5) lines, have flux values that are generally consistent with the basic, shock model conclusions of Smith *et al.* (1998). We can make an even stronger statement about excitation mechanisms, however, by looking at restrictions set by some of the other, predicted H_2 lines that are not seen. The PDR model most analogous to the model parameters we have, with n=3, g=3, predicts a strength for the 4-3 O(3) line at 3.3765 :m (one of the strongest discriminating H_2 lines) of $1.0x10^{-18}$ Watts/m^2. We set a limit from our analysis of the ISOSWS spectrum that is about 100

times fainter. Higher densities or lower uv flux values will only serve to increase the predicted line flux - and hence increase the discrepancy between theory and observation; for example, at g=4 and n=4, the discrepancy increases by a factor of three; the predicted flux will, however, drop by x2.7 when the uv field g increases but the density stays the same (e.g., the g=5, n=3 case). No reasonable combination explains the very small limit we set on the line, and we therefore conclude that pure PDR excitation cannot contribute in a significant way to the H_2 emission in the DR21 outflow.

3.2 *The Character of the Shock in DR21*

Our IRAC images, Figures 1, as well as the 2 :m image (Figure 2 overlay), show that the shocked H_2 emission in the outflow encompassed by the beam of ISOSWS includes many small knots. The calculated H_2 line brightness tables by Kaufman must therefore be corrected by appropriate, and somewhat uncertain, dilution factors when comparing absolute model flux predictions to the SWS observations presented in the tables. We can make quite reasonable estimates for clumping from the images, and with scaling arrive at a useful set of conclusions. Nearly all of the shock models predict much stronger fluxes than are observed; this can be seen from Figure 5b. The weakest model shown there, n=4, with v=30 kms^{-1} , has 4-band values of .1, .59, 3.3 and 6.8Jy; the observed IRAC flux densities are 0.058, 0.086, 0.44, and 1.08 Jy. If we choose a dilution factor of 10, however, a reasonable estimate (see Figure 2), the model values predicted for 3.6 :m, 4.5 :m, and 8.0 :m are reasonably close to those observed. These are the model values we have plotted in Figure 4 as asterisks, along with the observed IRAC fluxes (diamonds) , and the observed SWS line fluxes as they would appear to IRAC (squares).

The observed line fluxes as seen in the 3.6 :m band are, however, noticeably considerably stronger than that predicted by this scaled, best-fit shock model – by a factor of about 3.3. Adding other C-shock components from higher density regions could provide a solution, since at higher densities (as noted earlier) it is precisely the 3.6 :m, 4.5 :m fluxes which are most increased. Smith, Eisloffel, and Davis (1998) concluded that it was not possible to use a single shock model to explain the ISOSWS and ground-based lines they measured. Instead, they propose that a combination of C-type bow shocks with "wide flanks," together with localized extinction, can provide a consistent picture of the region. Alternatively, some component of low density PDR emission might accomplish the same thing, but would require a larger filling factor and a more careful analysis to explain the absence of the 4-3 O(3) line. The observed line fluxes as seen in the 3.6 :m band are, at the same time, noticeably weaker than the measured 3.6 :m band IRAC flux density of 58 mJy. We conclude that over 90% of the emission in Band 1 comes from warm dust, but we are unable to say more about the discrepancy between the SWS Band spectral data and the modeled H_2 emission in Band 1. ISOSWS did not take a full scan across the Band 1 interval of ~3.2 :m to 3.9 :m, but partial range scans exist in TDT 04402144 and others, and they give an rms baseline fit to the continuum of 87 ± 15 mJy. This value is just barely consistent with the measured 3.6 :m flux density of 58 mJy (Table 1), but given the uncertain calibration of the spectral scan continuum, which among other things has numerous wavelength coverage gaps, we believe it is adequately in agreement. We conclude that a combination of C-shocks provides a reasonably accurate explanation for the IRAC observations, with continuum dust emission dominating in the 3.6 :m band.

3.4 *The Character of the ISM in DR21 as Determined by IRAC*

Up to now we have analyzed the outflow in the region of the observed ISOSWS beam treated as an averaged whole. There is every reason to suspect, however, that additional details of the shock's structure can be revealed in the relative IRAC colors of the various knots and filaments. Figure 7a shows an IRAC color-color plot containing all of the pixels in the giant outflow (green points; given in magnitudes, in order to be most useful for comparison with point-source colors), and in the surrounding, unshocked nebulosity (blue crosses). The uncertainties in the colors of the fainter, diffuse nebulosity are larger than those in the bright knots, but our conclusions (below) are unchanged.

The colors of the emission of the outflow itself form a narrow locus of points stretching from a [3.6 - 4.5] color of 1.5mag in the top left of the color-color plot, down to a [5.8 - 8.0] color of 1.8 in the lower center. This locus is roughly the same as that produced by shocked H_2 lines alone, with preshock density of $1x10^4$ cm^{-3}, when the range of velocities varies from 20 - 40 kms^{-1} ; the top-most left portion corresponds to those lines originating from the fastest material. When the outflow is subdivided in smaller regions and their colors are separately considered, it is apparent that this range of colors is roughly the same in each zone. It is already clear from the work of Smith, Eisloffel, and Davis that multiple shock components are present; the variable colors across the flow simply confirm that complex and changing conditions are present.

There is one region in the outflow that is different from the others: the faintest part of the outflow – viz., the region at the western tip – is lacking in the reddest [3.6 - 4.5] gas whose color lies between about 0.6 and 1.2 mag in the other regions. We do not have spectra of the western tip, but we note that decreasing the preshock velocity from 40 kms^{-1} to 25 kms^{-1} will decrease the cumulative line flux ratio in these Bands in the most probable, low density case, by a factor of ~5. It does so largely by reducing the 4.5 :m band line emission; increasing the density by a factor of ten can accomplish about the same thing in the higher velocity cases. Our spectrum of the eastern portion of the outflow shows that Band 1 is dominated completely by dust emission. If that temperature is roughly constant across the outflow, then the 4.5 :m band H_2 line variations will control the [3.6 - 4.5] color variations. The flux from this region is admittedly quit weak in comparison with other regions, and also susceptible to contamination from surrounding nebulosity, but we argue nevertheless from the IRAC images that, on average, a slower, higher density shock is exciting the gas at the tip of the outflow.

In general, red IRAC nebulosity in the [5.8 - 8.0] color is due to strong 8 :m PAH emission. The DR21 outflow, however (at least in the bright easternmost portion studied by ISOSWS) has no sign of the characteristic PAH lines in these bands, and the bands are dominated by their H_2 emission lines. Just as slower shocks are much redder in the [3.6 - 4.5] color, so too they are redder in the longer wavelengths. Lowering the density will also make them appear redder at long wavelengths. Therefore we conclude that the concentration of points around [5.8 - 8.0] =1.7, especially in the outflow tip, is not a measure of increased PAH emission, but is consistent with the notion of a slower, higher density shock.

The background nebulosity, away from the massive strong outflow, is also of considerable interest, and we have also examined its IRAC colors. Figure 7b plots the colors of the non-outflow nebulosity. The IRAC images away from the outflow are obviously less green in appearance, meaning less strong H_2 emission in Band 2. Since the total flux densities are also much smaller, we have averaged these nebular regions over much larger areas than were used in the outflow itself. All of the non-outflow, nebulous regions are characterized by very modest reddening in the 3.6 :m and 4.5 :m bands -- typically a color less than [3.6 - 4.5] < 0.4mag; this is in contrast to values of 1.0 or greater in the outflow region. Red [3.6 - 4.5] colors are as strong an indicator of shock activity as is strong 4.5 :m emission. In contract, the [5.8 - 8.0] colors of the diffuse nebulosity are virtually indistinguishable from the average colors in the outflow itself. Within the diffuse material there is a slight tendency for faint material to be even redder than brighter nebulosity, perhaps suggesting that uv, which excites the PAH emission, plays a more dominant role in these regions. Li and Draine (2001) provide detailed quantitative models for the ISM in which they include PAH, silicate grain, and carbonaceous grain emission. Their Table 5 provides estimated, normalized flux densities for a range of seven values of the UV radiation field strength, χ_{MMP} , between 0.3 and 10^4 . The IRAC colors of all these seven scenarios are about the same: [3.6 - 4.5] ≈ –.35; [5.8 - 8.0] ≈ 2.1. The points are considerably bluer in [3.6 - 4.5] , by a factor of at least 60%, than all but the bluest of nebular regions in our image; the band [5.8 - 8.0] color is in good agreement with our observations. A much more complete discussion of the IRAC properties of the ISM, including a more detailed analysis of the ISM in the DR21 region, will be presented in Hora *et al.* (2006, in prep.).

4. CONCLUSIONS

Spitzer IRAC color images of star formation regions, typically coded with the 4.5 :m band as green, often show dramatic swaths of green nebulosity. In the case of the massive outflow in DR21, that "green monster" is produced almost entirely by the lines of shocked H_2. Not only is the H_2 flux in the 4.5 :m band strong in the region of the outflow, it is large in the 4.5 :m band (but only in the 4.5 :m band) compared to all the other normally considered nebular emission mechanisms. That is why (after scaling and correcting for bright point sources) the composite IRAC images of outflows are green: the 5.8 :m and 8.0 :m bands typically contain bright PAH emission elsewhere in the field which, when scaled down so as not to overpower the color image, decreases the outflow flux values much below the contribution from the 4.5 :m band which lacks these other bright features.

The ISOSWS spectra of the DR21 western outflow lobe have allowed us to determine not only that H_2 is the overwhelming contributor to the outflow emission, they also enable us (in agreement with earlier analyses) to conclude that some combination of modest velocity C-shocks in a medium whose preshock density is between 10^3 and 10^4 cm^{-3} is the mechanism responsible.

DR21 is an extreme case of an outflow from massive star formation. Nonetheless these results indicate that IRAC images can be a powerful detector of – and diagnostic for – shocked outflows caused by star formation activity throughout our galaxy, and in other nearby galaxies as well. It remains to be determined the extent to which the ~140 H_2 emission lines across the IRAC bands contribute to the 4.5 :m band flux densities seen in other star formation regions – or for that

matter in other bright nebulae, like planetaries, objects which are already known to be strong H_2 emitters. Typically only about twenty five dominate the IRAC bands in shocks, nine of them falling into the 4.5 :m band; ISOSWS saw the strongest of these latter nine lines, the 0-0 S(9) line, and only one of the next two strongest lines (which are 3 to 30 times weaker). Sensitive IRAC images, with their "green monster" nebulosities, have made it easy for scientists to spot small regions of the 4.5 :m band activity in otherwise large and complex fields. While the *Spitzer* IRS spectrometer cannot see the H_2 lines below 5 :m, its sensitive performance ought to enable a self-consistent picture to emerge from the other, longer wavelength H_2 lines that do fall in its windows.

We have not only found that the H_2 emission is strong – we have found that the continuum emission in this outflow is very weak. The implications, to be discussed further in the larger context of the DR21 star formation complex and sources (Smith *et al.* 2006), is that there are neither much dust nor hot PAH molecules abundant in this outflow.

IRAC color-color diagrams of the emission from regions across the outflow confirm the conclusions from the individual band flux analyses. In particular, the short wavelength colors in the flow are consistently redder than are the colors of the non-outflow, non-shocked ISM. Combined with shock models, the colors indicate that the shock at the western tip is likely to involve slower, denser material. The colors of the background nebulosity, away from the massive strong outflow, are characterized by very modest reddening between the 3.6 :m and 4.5 :m bands. They are mild disagreement with theoretical predictions of for ISM colors in both [3.6 - 4.5] and [5.8 - 8.0] colors.

The overall results indicate that IRAC images can be a powerful indicator of outflows caused by star formation activity. The results suggest IRAC color-color diagnostic diagrams for the nebulosity in star formation regions may sometimes need to take into account the possible influence of these strong H_2 emission lines, especially in cases when a large, extended emission is seen around an optically thick point source.

We gratefully thank Mark Wolfire and Michael Kaufman for providing us with their latest calculations of the H_2 line strengths. We also thank Chris Davis for providing unpublished data on his 2 :m H_2 images. HAS acknowledges partial support from NASA Grant NAG5-10654. This work is based in part on observations made with the *Spitzer* Space Telescope, which is operated by the Jet Propulsion Laboratory, California Institute of Technology under NASA contract 1407. Support for the IRAC instrument was provided by NASA through Contract Number 960541 issued by JPL. This work is also based in part on observations made with ISO, an ESA project with the participation of NASA and ISAS.

REFERENCES

Butt, Y.M, *et al.* 2003, ApJ, 597, 494

Cabrit, S., and Bertout, C. 1986, ApJ, 307, 313

Chandler, C.J., Gear, W.K., and Chini, R. 1993, MARAS, 260, 337

Chandler, C. J., Carlstrom, J. E., Scoville, N. Z., Dent, W. R. F.,Geballe, T. R. 1993, ApJ, 412, L71

Church well, E., et al. 2004, ApJSupp 154, 322

Cyganowski, C.J., Reid, M.J., Fish, V.L., and Ho, P.T.P. 2003, ApJ, 596, 344

Davis, C.J., and Smith, M.D. 1996, A&A, 310, 961

Fernandes, A.J.L., Brand, P.W.J.L., and Burton, M.G. 1997, MARAS, 290, 216

Garden, R.P., and Carlstrom, J.E. 1992, ApJ, 392, 602

Garden, R.P., Russell, A.P.G., and Burton, M.G. 1990, ApJ, 354, 232

Garden, R.P., Geballe, T.R., Gatley, I., and Nadeau, D. 1986, MNRAS, 220, 203

Garden, R.P., Geballe, T.R., Gatley, I., and Nadeau, D. 1991, ApJ, 366, 474

Geballe, T.R., and Garden, R.P. 1990, ApJ, 365, 602

Geballe, T.R., and Garden, R.P. 1990, ApJ, 317, L107

Kaufman, M.J., Wolfire, M.G., and Hollenbach, D.J. 2005 (preprint)

Kaufman, M.J., and Neufled, D.A. 1996, ApJ, 456, 611

Li, A., and Draine, B.T. 2001, ApJ, 554, 778

Marston, A.P. *et al.* 2004, ApJSupp, 154, 333

Rosenthal, D., Bertoldi, F., and Drapatz, S. 2000, A&A, 356, 705

Smith, M. D., Eisloffel, J., and Davis, C.J. 1998, MARAS, 297, 687

Smith, M.D., and Rosen, A. 2005, 357, 1370

van Dishoeck, E.F., Wright, C.M., Cernicharo, J., Gonzalez-Alfonso, E., de Graauw, T., Helmich, F.P., and Vendenbussche, B. 1998, ApJ, 502, L173

Wilson, T.L., and Mauersberger, R. 1990, A&A, 239, 305

Wolfire, M. G., Tielens, A. G. G. M., and Hollenbach, D. 1990, ApJ, 358, 116

Wright, C.M., Timmerman, R., and Drapatz, S. 1997, in Proc. First ISO Workshop on Analytical Spectroscopy, ed. A.M. Heras, K. Leech, N. R. Trams, & M. Perry (Noordwijk, ESA Publications Division) 311

Table 1a:
Fluxes of the ISOSWS observed H_2 Lines

Line ID	wavelength :m	Observed flux (W/m^2)	flux contribution to IRAC bands
0-0S(4)	8.025	4.80E-15	3.74E-01
0-0S(5)	6.9069	1.15E-14	7.55E-01
1-1S(7)	5.8075	1.16E-16	9.06E-03
0-0S(7)	5.5081	5.35E-15	4.15E-01
1-1S(9)	4.9535	1.45E-16	9.97E-03
0-0S(9)	4.694	1.81E-15	1.24E-01
0-0S(11)	4.181	8.82E-16	5.81E-02
1-0 O(5)	3.235	5.40E-16	2.49E-03

Table 1b:
IRAC flux (Jy): inferred H_2 Lines, and observed flux densities

		H_2 observed fluxes (from ISOSWS)	Observed IRAC fluxes (in the ISOSWS beam)
	center wavelength		
Band 1	3.6 :m	2.49E-03	0.058
Band 2	4.5 :m	.192	.086
Band 3	5.8 :m	.424	.44
Band 4	8.0 :m	1.13	1.08

Figure 1: The IRAC Band 1 (3.6 :m - blue), Band 2(4.5 :m - green), Band 4(8.0 :m - red) composite image of DR21(main). The ISOSWS 14"x20" field is shown outlines in black.

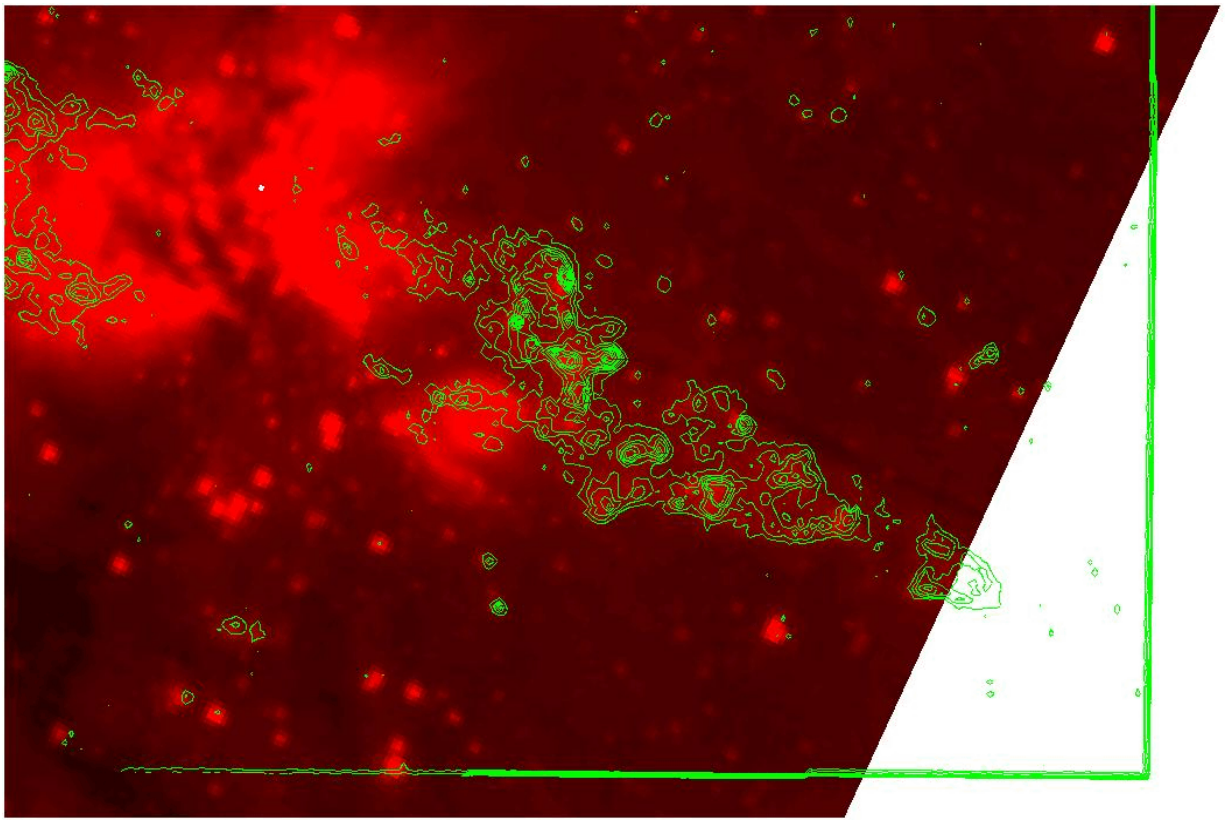

Figure 2: IRAC 4.5 μm band image, with overlaid contours of the K-band H_2 1-2 S(1) line emission map (from Chris Davis, private comm.) Note the one-to-one correspondence of the H_2 peaks with the bright 4.5 μm band knots.

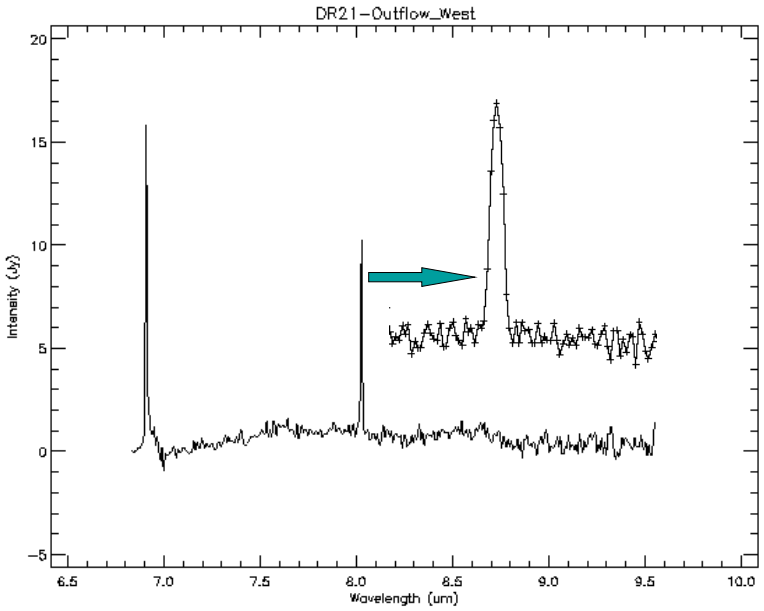

Figure 3a: A portion of the ISOSWS scan of the outflow. It shows the 0-0 S(4) emission line; the inset shows a zoom on this line. Note the very low continuum emission in the outflow.

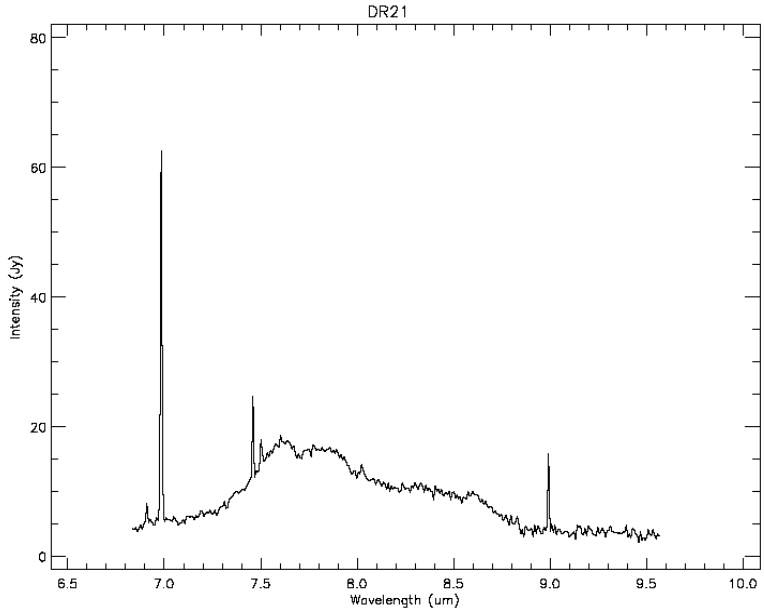

Figure 3b: In dramatic contract to Fig 4a, the ISOSWS spectrum of DR21 at the peak of the dust cloud shows strong continuum and PAH features, as well as lines of H_2, and atomic lines. The 0-0 S(4) line at 8.025 μm is visible, but not at all prominent.

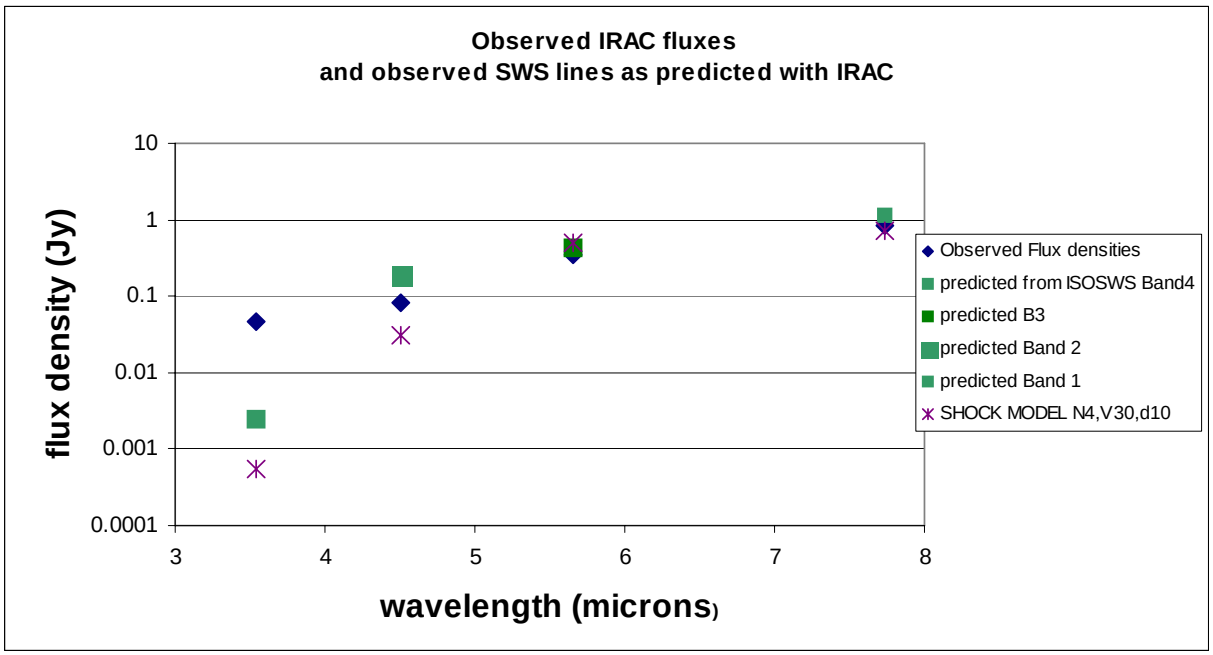

Figure 4: IRAC vs. ISOSWS observations. The observed IRAC flux densities in the DR21 outflow, measured in the same beam as the ISO SWS spectral observations, are plotted as blue diamonds; the observed SWS line fluxes per band, converted to IRAC flux densities, are also plotted a green squares. The observed H_2 line intensities account for nearly all of the flux seen by IRAC in the 4.5 :m, 5.8 :m, and 8.0 :m bands. The asterisks show the fit of best approximate model: a shock with preshock density of 10^4 cm^{-3} and a shock velocity of 30 kms^{-1} , assuming a dilution factor of ten.

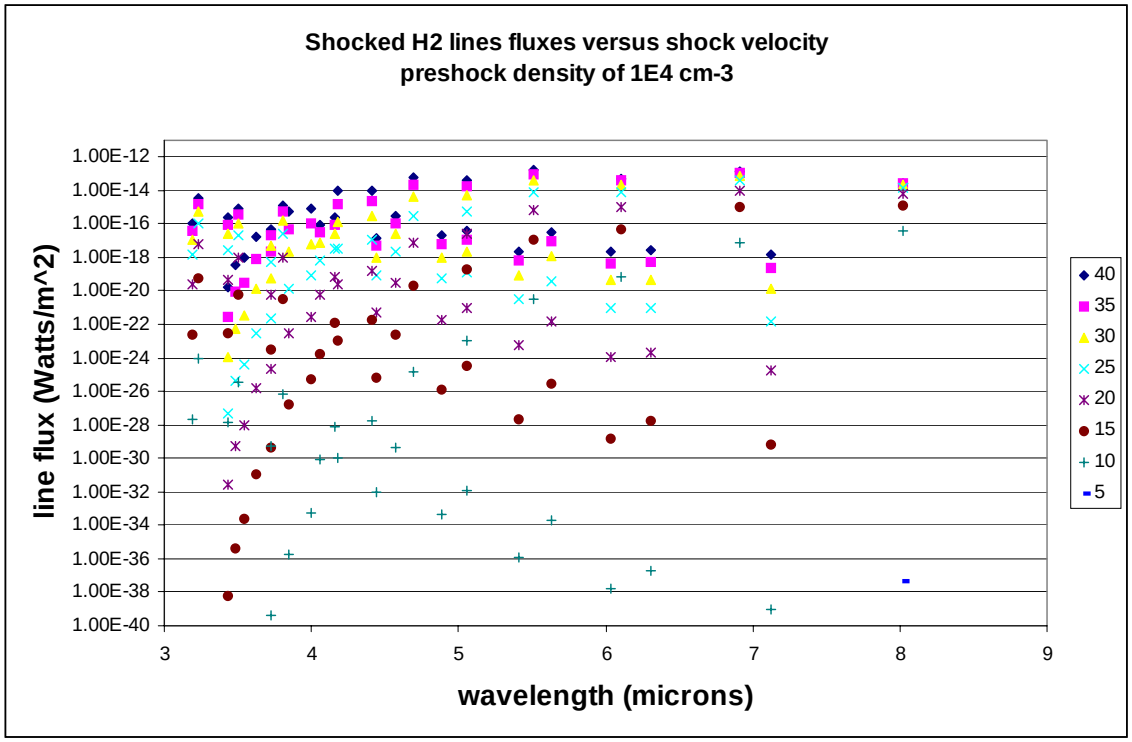

Figure 5a

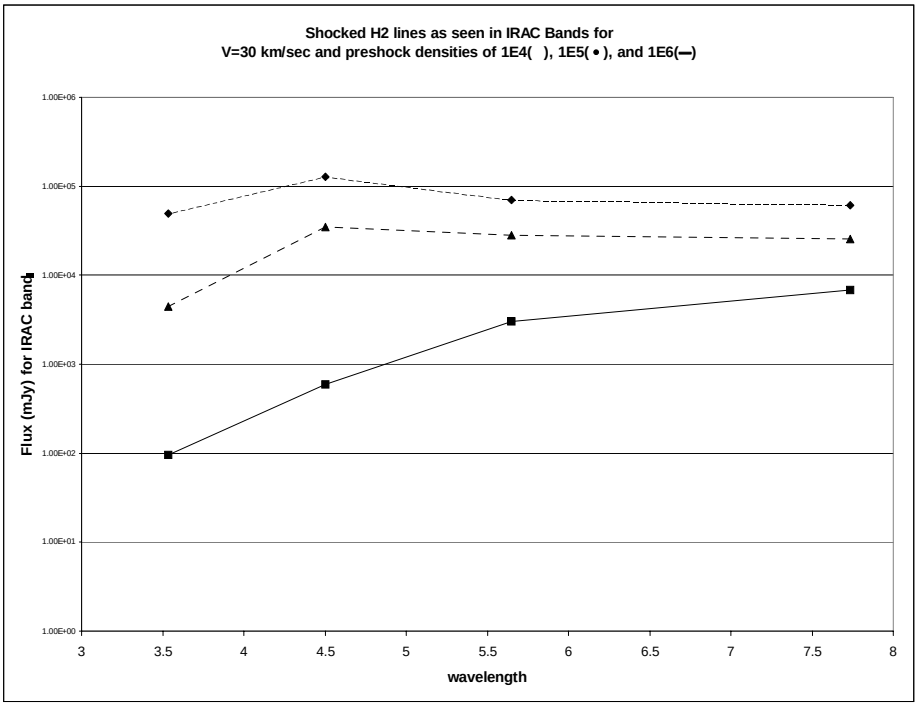

Figure 5b

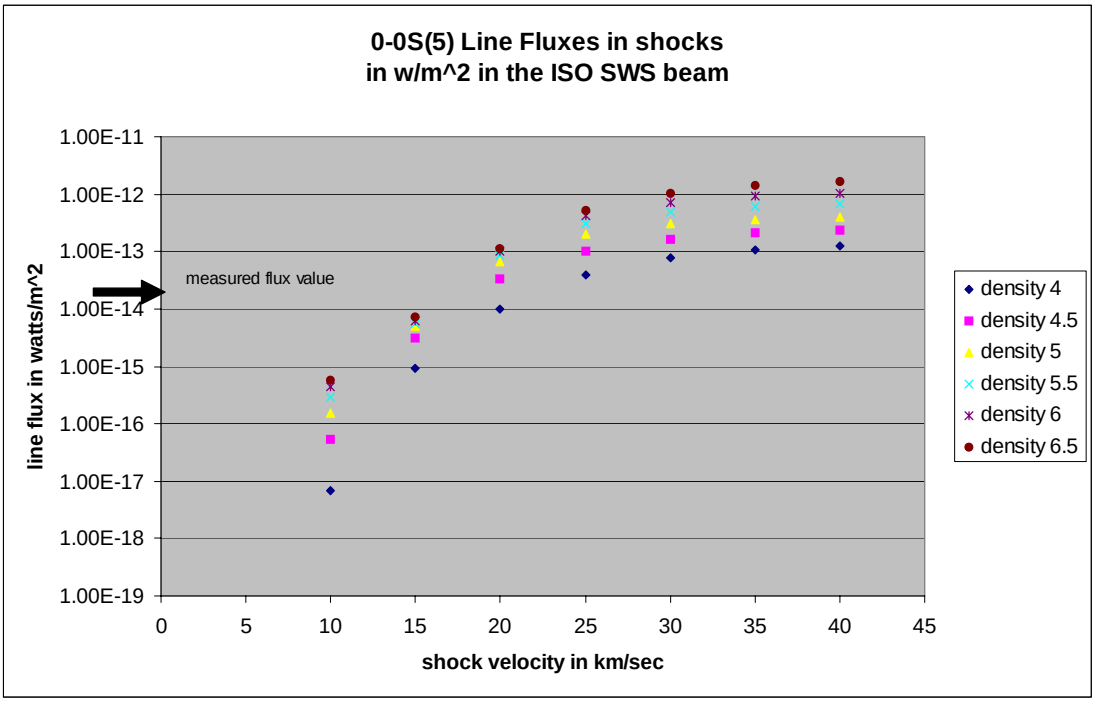

Figure 5c

Figure 5a: For the case of a preshocked density of 1E4, a plot of the brightest shocked lines versus shock velocity (in kms^{-1}).

Figure 5b: The cumulative contribution to the flux in the IRAC bands of shocked H_2 lines for the cases of three different preshock densities (1E4, 1E5, and 1E6 cm^{-3}), and with a preshock velocity of 30 kms^{-1}. (No dilution factors are used .)

Figure 5c: The diagnostic H_2 line 0-0 S(5) at 6.909 ：m (no dilution factor is used). This line is seen strongly in the DR21 outflow at a measured flux in the ISOSWS beam of $1.1x10^{-14}$ W/m^2.

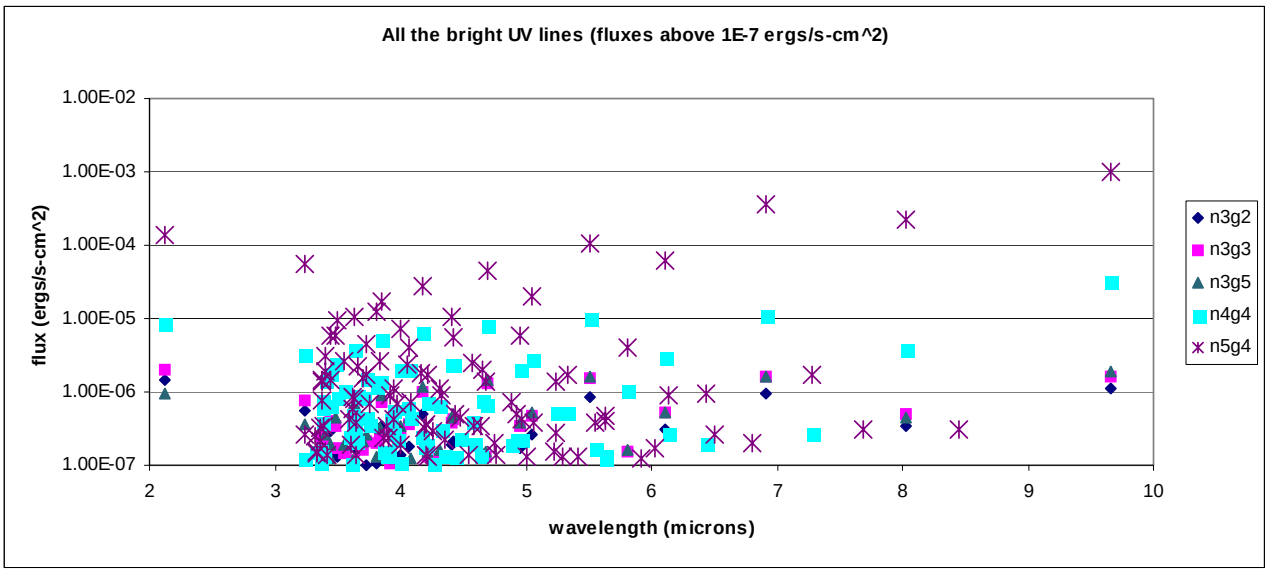

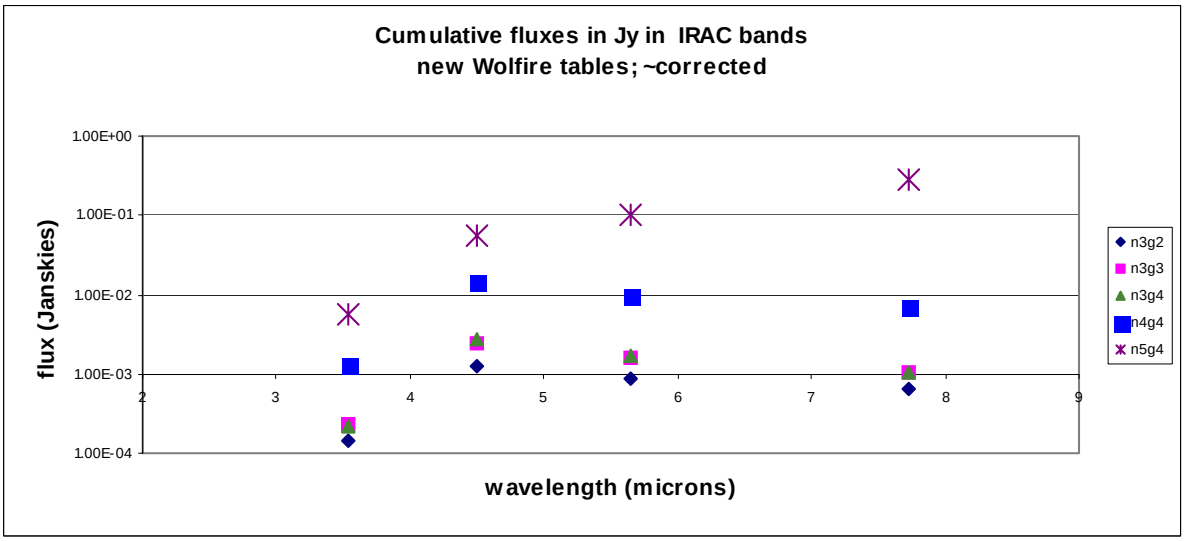

Figure 6a: The brightest 90% of the H_2 lines in the PDR excitation models (Wolfire, private comm.)

Figure 6b: The cumulative contribution to the flux in the IRAC Bands of the uv excited H_2 lines for five different cases of density and UV field.

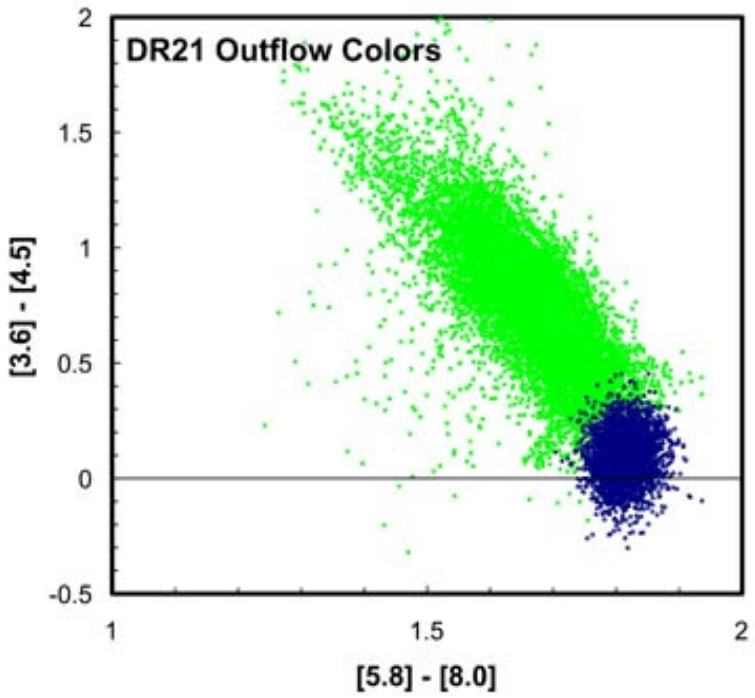

Figure 7: IRAC colors of the shocked outflow nebulosity (green points) and surrounding nebulosity (blue crosses). The points correspond to individual IRAC pixels in the outflow. Analysis by subregion finds that all parts of the flow except one have roughly the same range of pixel colors; the western-most tip is lacking the red [3.6]-[4.5] points with values above 0.6. The blue crosses correspond to pixels away from the outflow, in the general DR21 nebulosity. The expected IRAC colors of diffuse nebulosity from the Li and Draine (2001) ISM models fall in the plot around the value (2.1, -0.35), appreciably removed from the observed locus in DR21.